

# Threshold behavior in spin lasers: Spontaneous emission and nonlinear gain

Gaofeng Xu,<sup>1,2,\*</sup> Krish Patel,<sup>2</sup> and Igor Žutić<sup>2,†</sup>

<sup>1</sup>*Department of Physics, Hangzhou Dianzi University, Hangzhou, Zhejiang 310018, China*

<sup>2</sup>*Department of Physics, University at Buffalo, State University of New York, Buffalo, NY 14260, USA*

A hallmark of spin-lasers, injected with spin-polarized carriers, is their threshold behavior with the onset of stimulated emission. Unlike the single threshold in conventional lasers with unpolarized carriers, two thresholds are expected in spin lasers. With the progress in scaled-down lasers and the use of novel two-dimensional materials it is unclear if the common description of spin lasers assuming a negligible spontaneous emission and linear optical gain remains relevant or even how to identify the lasing thresholds. Our rate-equation description addresses these questions by considering a large spontaneous emission and a nonlinear optical gain. We provide a transparent approach and analytical results to explore the resulting threshold behavior, its deviation from the prior studies, as well as guide future spin-lasers as a versatile platform for spintronics beyond magnetoresistance.

The use of lasers in practical applications usually reflects their highly-controllable nonlinear coherent response [1–3]. With a current injection required for the onset of lasing, there is a striking change from incoherent to coherent emitted light that can be described by the Landau theory of second-order phase transitions [4, 5]. However, in scaled-down lasers, a large contribution of the spontaneous emission blurs this transition and even a thresholdless lasing is possible [6–10], while offering advantages for optical interconnects, imaging, sensing, and biological applications [11].

Through conservation of angular momentum, injecting spin-polarized carriers in lasers offers control of the helicity of emitted light and room-temperature spintronic applications, beyond magnetoresistance [12–18]. Such spin lasers [22–42] can exceed the performance of the best conventional counterparts (with spin-unpolarized carriers) as well as motivate emerging device concepts, from spin interconnects [19, 20] to phonon lasers [21]. Typically, spin lasers are realized as a vertical cavity surface emitting laser (VCSEL) [3], shown in the inset of Fig. 1.

The rate equations for spin lasers [24–26, 43–46] often rely on a linear gain model, common to bulk materials, despite the nonlinear gain dependence on the carrier density [47–50]. Since the carrier density dependence of the gain in systems of reduced dimensionality, such as quantum wells, are more accurately described by a logarithmic function [1–3, 50], here we consider usually overlooked effects of spontaneous emission and logarithmic gain on the threshold behavior of spin lasers. With a general gain model, the rate equations can be expressed as [43, 44],

$$\frac{dn_{\pm}}{dt} = J_{\pm} - g_{\pm}S^{\mp} - (n_{\pm} - n_{\mp})/\tau_s - R_{sp}^{\pm}, \quad (1)$$

$$\frac{dS^{\pm}}{dt} = \Gamma g_{\mp}S^{\pm} - S^{\pm}/\tau_{ph} + \beta\Gamma R_{sp}^{\mp}, \quad (2)$$

where  $n_{\pm}$  are the densities of spin-up (down) + (–) electrons, with a spin-relaxation time  $\tau_s$ . Since holes have much shorter spin-relaxation times than those of electrons in semiconductor quantum wells [12], only the electrons are spin polarized, while charge neutrality yields

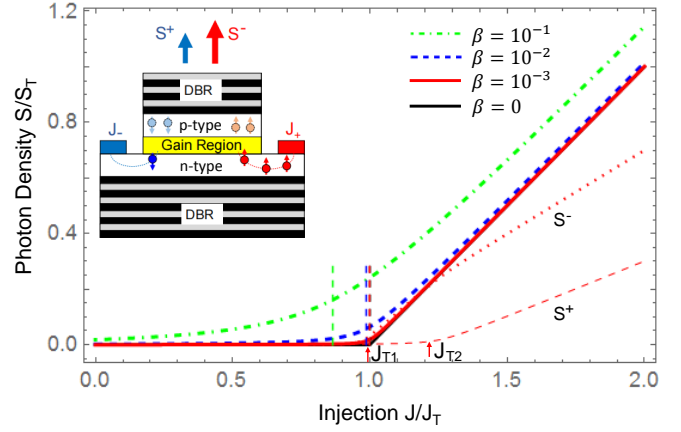


FIG. 1. Photon density  $S$  as functions of injection  $J$  for  $\beta = 0, 10^{-3}, 10^{-2}, 10^{-1}$ , with the vertical lines indicating the threshold injection  $J_T(\beta)$ , respectively. Helicity-resolved  $S^{\pm}$  are shown as a function of injection with polarization  $P = 0.2$  for  $\beta = 10^{-3}$  and the corresponding thresholds  $J_{T1,2}$  (arrows). The photon densities and injection are normalized by  $J_T \equiv J_T(0)$  and  $S_T = S(2J_T)$ . Inset: A schematic of a spin laser formed by a gain region,  $p$ - and  $n$ -type semiconductor layers, and distributed Bragg reflectors (DBR), with injection of different spins (here  $J_+ > J_-$ ,  $J \equiv J_+ + J_-$ ) and circularly-polarized emission with  $S^- > S^+$ .

the densities of holes  $p_{\pm} = (n_+ + n_-)/2$ .  $J_{\pm}$  are the injection rates of spin-up (down) + (–) electrons, with the polarization  $P = (J_+ - J_-)/J$ .  $S^{\pm}$  are the photon densities of positive (+) and negative (–) helicity. The spontaneous recombination of carriers can be expressed in a linear form as  $R_{sp}^{\pm} = n_{\pm}/\tau_r$ , characterized by a carrier recombination time  $\tau_r$  [43, 51, 52]. The optical gain can have various dependence on the carrier density. In a simple linear model, the spin-dependent gain takes the form  $g_{\pm} = g_0(n_{\pm} + p_{\pm} - n_{tran})$ , with  $g_0$  the gain parameter and  $n_{tran}$  the transparency carrier density.  $\Gamma$  is the optical confinement factor and  $\tau_{ph}$  is the photon lifetime in the cavity. The spontaneous emission factor  $\beta$  characterizes the fraction of spontaneous emission coupled to the lasing mode. For a typical spin laser,  $\beta \sim 10^{-5} - 10^{-3}$  [25, 26], justifies the  $\beta = 0$  approximation.

The threshold behavior of (spin) lasers without significant contribution from spontaneous emission has been well established. When  $\beta = 0$ , the steady-state solution of the rate equations without spin injection ( $J_+ = J_-$ ) gives the threshold carrier density  $n_T = n_{tran} + 1/(\Gamma g_0 \tau_{ph})$  and steady-state photon density  $S = \Gamma \tau_{ph}(J - n_T/\tau_r)$ , which leads to the threshold injection  $J_T = n_T/\tau_r$  [43].

However, the spontaneous emission is in general not

$$S(J) = \frac{1}{2}\Gamma\tau_{ph}(J - n_T/\tau_r) + \frac{\sqrt{[\Gamma g_0 \tau_{ph}(J\tau_r - n_T) + \Gamma g_0 \tau_{ph} n_T \beta - \beta]^2 + 4\Gamma g_0 \tau_{ph} \tau_r J \beta + (\Gamma g_0 n_T \tau_{ph})\beta}}{2g_0 \tau_r}. \quad (3)$$

In Fig. 1 we see that, with increasing  $\beta$ , the originally abrupt transition from nonlasing to lasing region gradually becomes smoother, which makes the definition of lasing threshold challenging.

To investigate the threshold behavior for lasers with

negligible. In scaled-down lasers, due to their reduced cavity sizes and the Purcell effect [53], there are reports of significantly enhanced spontaneous emission factors up to  $\beta \sim 0.1$ , which significantly changes the threshold behavior and even thresholdless lasers are possible [6–10]. To explore the effect of  $\beta$  on the lasing threshold, we obtain an analytical relation between  $S$  and  $J$  by solving the steady-state rate equations with  $\beta \neq 0$ ,

$\beta \neq 0$ , we examine the derivatives of  $S(J)$  [54, 55]. The first derivative,  $S'(J)$ , grows gradually in the transition region, reflecting the increasing rate of the photon density. However, by obtaining the second derivative

$$S''(J) = \frac{2g_0^2 n_T (1 - \beta) \beta \Gamma^3 \tau_{ph}^3 \tau_r}{\left[4g_0 \beta \Gamma \tau_{ph} \tau_r J + (\beta - g_0 n_T \beta \Gamma \tau_{ph} + g_0 \Gamma \tau_{ph} (n_T - \tau_r J))^2\right]^{3/2}}, \quad (4)$$

we can identify a characteristic single peak as a function of  $J$ . This is shown in the inset of Fig. 2 for  $\beta = 0.01$ . For a smaller  $\beta$ , the peak becomes sharper, and in the limit of  $\beta \rightarrow 0$ , the peak becomes a Dirac  $\delta$ -function. With  $\beta \neq 0$ , the lasing transition occurs at a range of injection centered at the peak. The peak position of  $S''(J)$  represents the fastest change in the increasing rate  $S'(J)$ . Therefore, for  $\beta \neq 0$ , the injection corresponding to the peak of  $S''(J)$  can serve as the representative value of the lasing threshold, which is given by

$$J_T(\beta) = n_T/\tau_r - \beta(2n_T - n_{tran})/\tau_r, \quad (5)$$

showing a linear decrease with  $\beta$ , as indicated by the vertical lines in Fig. 1 for a few cases and specifically given by the dashed line in Fig. 2. We note that if

$$\beta \geq 1/(2 - n_{tran}/n_T), \quad (6)$$

the peak feature of  $S''(J)$  would be lost and therefore the threshold vanishes, i.e., the laser becomes thresholdless in this definition. In Figs. 1 and 2, the injection is normalized by its threshold  $J_T$  at  $\beta = 0$ , and the photon densities are normalized by  $S_T = S(2J_T) = \Gamma n_T \tau_{ph}/\tau_r$ . Unless otherwise specified, the parameters in our calculations are:  $\Gamma = 0.02$ ,  $n_{tran} = 3.0 \times 10^{12} \text{ cm}^{-2}$ ,  $\tau_r = 200 \text{ ps}$ ,  $\tau_{ph} = 0.5 \text{ ps}$  [56],  $\tau_s = 200 \text{ ps}$ ,  $g_0 = 60 \text{ cm}^2 \text{ s}^{-1}$ .

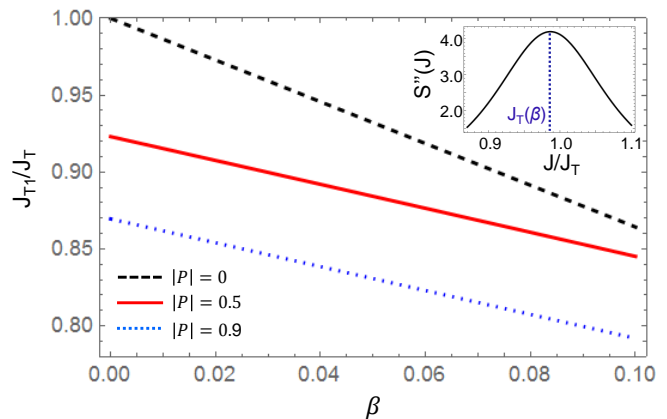


FIG. 2. Dependence of  $J_{T1}/J_T$  on  $\beta$  for injection with polarization  $|P| = 0, 0.5$ , and  $0.9$ .  $J_{T1}$  is normalized by its threshold  $J_T$  at  $P = 0$  and  $\beta = 0$ . Inset: the second derivative  $S''(J)$  for  $\beta = 0.01$ , with the peak position, i.e., threshold  $J_T(\beta)$ , marked by the vertical line. The photon density  $S$  is normalized by  $S_T$ .

While our definition of a threshold relies on the experimentally measurable kink in the light-injection curves, other choices also exist in conventional lasers ( $P = 0$ ). For example, one used in microcavity lasers assumes that  $S$  represents the density inside of the the gain region of

a volume  $V$  and that at threshold the photon number in the lasing mode is  $SV = 1$  [57]. Both definitions share similarities,  $J_T(\beta \neq 0) < J_T(\beta = 0)$ , but in our case  $J_T$  is linearly reduced with  $\beta$  (Fig. 2).

With various experiments on nano and microcavity spin lasers [36, 58], in which  $\beta$  exceeds previous values by several orders of magnitude [25, 26], there is an outstanding question about the influence of large spontaneous emission when  $P \neq 0$ . Due to the optical selection rules, light with different helicities  $S^\pm$  exhibit separate thresholds  $J_{T1,2}$  [26, 33] under spin injection, as shown in Fig. 1. Ignoring spontaneous emission ( $\beta = 0$ ), the first threshold of spin lasers can be obtained as [43]

$$J_{T1}(P) = \frac{1}{1 + |P|/(4\tau_r/\tau_s + 2)} J_T, \quad (7)$$

where the minimum threshold  $J_{T1}^{min} = (4\tau_r + 2\tau_s)/(4\tau_r + 3\tau_s)J_T$  is reached at  $|P| = 1$ , which gives  $J_{T1}^{min}/J_T = 2/3$  in the limit of long spin-relaxation time ( $\tau_s \gg \tau_r$ ) [33, 59]. For the recombination linear in  $n$ , threshold reduction is up to 1/3, smaller than the widely accepted theoretical limit 1/2 [24–26, 28]. This is because the spin-

dependent optical gain contains contribution from the spin-polarization of holes, the threshold reduction of 1/2 is attained for their infinite spin-relaxation time. However, consistent with typical III-V semiconductors [12], hole spin-relaxation times are much shorter than for electrons, and therefore  $p_+ = p_-$  is assumed in Eqs. (1) and (2), which diminishes the maximum threshold reduction.

Analytical solutions of the steady-state rate equations with spin injection are generally unavailable. However, in the regime of a single-mode lasing  $J_{T1} < J < J_{T2}$ , the photon density of the nonlasing mode with spin-disfavored helicity is relatively small, e.g.,  $S^- \ll S^+$ . Therefore, assuming  $S^- \approx 0$  is accurate and simplifies the steady-state equations. Under this approximation, the analytical solutions for  $S^+(J)$  and  $S''(J)$  can be obtained, which are qualitatively the same as for conventional lasers [see Eq. (4)], only with more complicated expressions. Therefore, we propose that the same definition of  $J_{T1}$  as the peak position of  $S''(J)$  developed in conventional lasers can be extended to spin lasers. Despite the complexity of the full expression of  $J_{T1}$ , it is instructive to look at its simplification in the limit of long spin-relaxation times ( $\tau_s \gg \tau_r$ )

$$J_{T1}(P, \beta) = \frac{4 + 2|P| - (7 + 5|P|)\beta + \Gamma g_0 \tau_{ph} n_{tran} (1 - \beta) [4 + 2|P| - (1 - |P|)\beta]}{\Gamma g_0 \tau_{ph} \tau_r [2 + |P| - (1 - |P|)\beta/2]^2}, \quad (8)$$

which reduces to Eq. (7) for  $\beta = 0$  in the limit of  $\tau_s \gg \tau_r$ .

To illustrate the effect of spontaneous emission and polarization of injection, we show in Fig. 2 the dependence of  $J_{T1}$  on  $\beta$  for  $|P| = 0, 0.5$ , and  $0.9$ . The result for the conventional laser ( $|P| = 0$ ) is based on Eq. (5). We see that for all cases, the lasing thresholds decrease approximately linearly with  $\beta$ , while  $|P| \neq 0$  leads to a further threshold reduction. The decreasing rates for the spin-unpolarized and spin-polarized lasers are different. We note that the circular polarization of the emission would be reduced with increasing  $\beta$  due to a larger contribution from spontaneous emission, which could be partially compensated by a longer spin-relaxation time.

While a moderate spin relaxation time  $\tau_s = \tau_r = 0.2$  ns is used in Fig. 2, the threshold of spin lasers can be significantly influenced by  $\tau_s$ , as illustrated in Fig. 3, where the corresponding dependence of the threshold  $J_{T1}$  for  $\beta = 0$  and  $0.1$  is shown. The curves show a similar trend that, with small  $\tau_s$ ,  $J_{T1}$  approaches the threshold value of the corresponding conventional laser, while threshold reduction increases with  $\tau_s$ . This allows us to establish a steady-state picture and key trends of the threshold behavior of (spin) lasers, by combining our results for conventional and spin lasers with  $\beta = 0$  and  $\beta \neq 0$ . While the illustration here is given for  $\beta$  up to  $0.1$ , the observed

trends are also retained outside of this range.

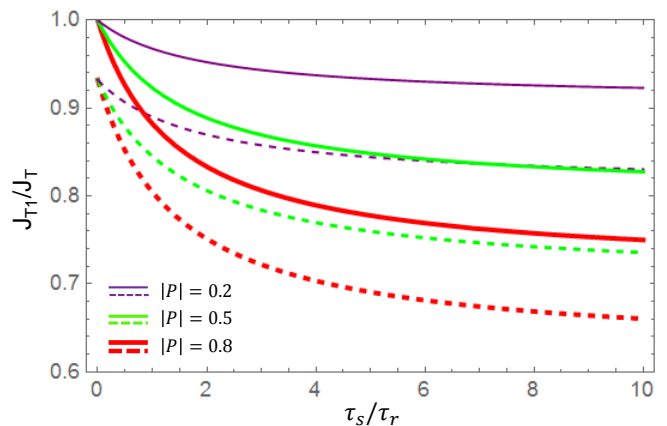


FIG. 3. Influence of the normalized spin relaxation time  $\tau_s/\tau_r$  on the normalized threshold  $J_{T1}/J_T$  for  $\beta = 0$  (solid),  $0.1$  (dashed) and  $|P| = 0.2, 0.5, 0.8$ .

So far, our rate equations have relied on a simple linear gain model, which is a good approximation in the vicinity of  $n_{tran}$  and for bulk-like materials [1, 2]. However, the optical gain is generally nonlinear, especially for low-dimensional gain regions and carrier densities far from  $n_{tran}$ , where the accuracy of a linear gain model declines. In contrast, a logarithmic gain model can accurately de-

scribe the nonlinearity of realistic gain curves, with effects such as gain saturation accounted for [1, 2, 50]. To describe the spin-dependent gain, we generalize a typical logarithmic gain model [1, 2] to obtain

$$g_{\pm}(n_{\pm}, p_{\pm}) = g'_0 n_{tran} \ln \frac{n_{\pm} + p_{\pm} + n_s}{n_{tran} + n_s}, \quad (9)$$

where  $n_s$  is a fitting parameter to be determined by the specific gain curve. For a better comparison, we make a connection between the gain models by matching the differential gain at  $n_{tran}$ , which leads to  $g'_0 = (1 + n_s/n_{tran})g_0$ . Here we set  $n_s = 0.1n_{tran}$  for the purpose of illustration. A comparison of linear and logarithmic gain curves is shown in the inset of Fig. 4, where the two curves coincide at  $n_{tran}$  and deviate from each other away from  $n_{tran}$ .

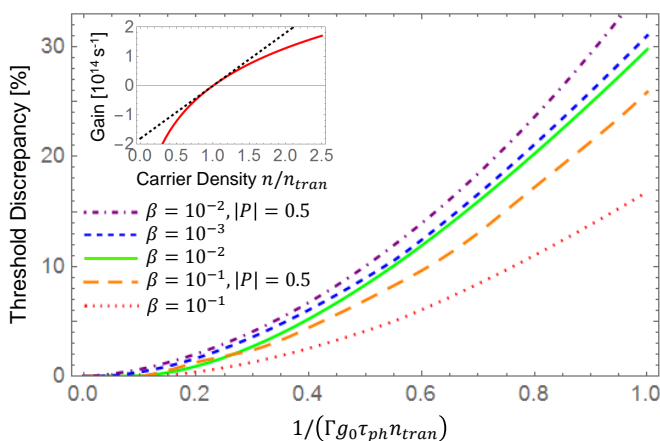


FIG. 4. The relative discrepancies in thresholds between linear and logarithmic gain models as a function of  $1/(\Gamma g_0 \tau_{ph} n_{tran})$  for  $\beta = 10^{-3}, 10^{-2}, 10^{-1}$  for conventional and spin lasers (with  $|P| = 0.5$ ). The inset shows a comparison of linear (dashed) and logarithmic gain curves (solid), with the carrier density normalized by  $n_{tran}$ .

For  $\beta = 0$ , the steady-state solutions with the logarithmic gain for conventional lasers are

$$n_T^{ln} = (n_{tran} + n_s) \exp[1/(\Gamma g'_0 n_{tran} \tau_{ph})] - n_s, \quad (10)$$

$$S^{ln} = \Gamma \tau_{ph} (J - n_T^{ln} / \tau_r), \quad (11)$$

which leads to the threshold injection  $J_T^{ln} = n_T^{ln} / \tau_r$ . Therefore, the threshold difference between logarithmic and linear gain is determined by the corresponding threshold carrier densities:  $J_T^{ln} - J_T^{lin} = (n_T^{ln} - n_T^{lin}) / \tau_r$ . An intuition can be gained by considering the regime  $(n_T^{ln} - n_{tran}) / n_{tran} \ll 1$ , i.e.,  $1/(\Gamma g'_0 n_{tran} \tau_{ph}) \ll 1$ , which allows an expansion of the exponential function in Eq. (10). The leading order approximation gives  $n_T^{ln} - n_T^{lin} \approx (n_{tran} + n_s) / [2(\Gamma g'_0 n_{tran} \tau_{ph})^2]$ , which suggests that in general  $n_T^{ln} > n_T^{lin}$  and thus  $J_T^{ln} > J_T^{lin}$ , with the difference largely dependent on the factor  $1/(\Gamma g'_0 n_{tran} \tau_{ph})$ . This can be understood since the logarithmic gain includes the gain saturation, and thus it has a lower gain value at the same carrier density above

$n_{tran}$  (see the inset of Fig. 4). Therefore, a larger  $n$  and thus  $J$  is needed to reach the lasing threshold.

Unlike the case of the linear gain, an analytical steady-state solution of  $S(J)$  with  $\beta \neq 0$  is no longer available due to the complexity of the logarithmic function. However, our analysis for the case of  $\beta = 0$  that the threshold discrepancy between linear and logarithmic gain models depends on the threshold carrier density can be extended. For simplicity and connection with linear gain models, we consider the dependence of the discrepancy on  $(n_T^{lin} - n_{tran}) / n_{tran} = 1/(\Gamma g_0 \tau_{ph} n_{tran})$  instead.

We show in Fig. 4 the relative discrepancy of threshold between logarithmic and linear gain  $(J_T^{ln} - J_T^{lin}) / J_T^{lin}$  as a function of  $1/(\Gamma g_0 \tau_{ph} n_{tran})$  for  $\beta = 10^{-3}, 10^{-2}$ , and  $10^{-1}$  for conventional and spin lasers (with polarization of injection  $|P| = 0.5$ ). For all cases, the discrepancy approaches to 0 in the limit of small  $1/(\Gamma g_0 \tau_{ph} n_{tran})$ . The relative discrepancy increases monotonically with  $1/(\Gamma g_0 \tau_{ph} n_{tran})$  and it is smaller with larger  $\beta$ . Moreover, the relative discrepancy in  $J_{T1}$  of spin lasers is greater than that of the respective conventional lasers. Therefore,  $1/(\Gamma g_0 \tau_{ph} n_{tran})$  is a characteristic quantity that indicates the accuracy of the linear gain model in calculating the lasing threshold. If  $1/(\Gamma g_0 \tau_{ph} n_{tran}) \ll 1$ , linear gain models agrees well with logarithmic models. Otherwise, their discrepancy becomes significant. A simple linear gain model often underestimates the lasing threshold due to the neglect of the gain saturation, and its accuracy can be inferred from the magnitude of the quantity  $1/(\Gamma g_0 \tau_{ph} n_{tran})$ .

While we have focused here on the steady-state response of spin lasers, our findings have broader implications and could guide the design of future scaled-down lasers, where both large spontaneous emission and nonlinear gain are expected to play important roles. For example, in the limit  $\beta = 0$ , it was found that threshold reduction also results in an enhanced modulation bandwidth [44], suggesting that with a large  $\beta$  a further threshold reduction could be desirable.

There is a growing interest to utilize optical anisotropy in spin lasers, such as the high birefringence [39, 41, 49, 60–66], to reach ultrafast operation, faster than the best conventional lasers [42]. Even though such efforts focus on quantum-well based lasers (where a nonlinear optical gain is expected) and scaling them down [58], their current description relies on a widely-used spin-flip model [67–70]. While that approach includes optical anisotropies, the assumed linear gain and  $\beta = 0$  limits its predictive power to elucidate scaled-down spin lasers. Alternatively, optical anisotropy can be tailored in vertical external cavity surface emitting lasers, which are another promising platform to implement spin lasers [35, 71, 72], where it would also be important to study the role of a nonlinear gain and large  $\beta$ .

Beyond the spin lasers, the question of the threshold behavior continues to also be debated in conventional

counterparts. A growing class of atomically-thin materials, such as transition metal dichalcogenides, were suggested as promising for spin lasers [46] and later used as the gain region in conventional lasers with a large  $\beta$  [73, 74]. However, within analyzing a linear optical gain model, these experiments were argued not to have achieved a lasing threshold [75], prompting a need for both additional experiments as well as further theoretical analysis which may benefit from our findings.

This work has been supported by the NSF ECCS-1810266 and 2130845. We thank N. C. Gerhardt for valuable discussions.

## AUTHOR DECLARATIONS

### Conflict of interest

The authors have no conflicts to disclose.

### DATA AVAILABILITY

The data that supports the findings of this study are available within the article.

---

\* xug@hdu.edu.cn

† zigor@buffalo.edu

- [1] S. L. Chuang, *Physics of Optoelectronic Devices*, 2nd ed. (Wiley, New York, 2009).
- [2] L. A. Coldren, S. W. Corzine, and M. L. Mašović, *Diode Lasers and Photonic Integrated Circuits*, 2<sup>nd</sup> Edition (Wiley, Hoboken, 2012).
- [3] *VCSELs Fundamentals, Technology and Applications of Vertical-Cavity Surface-Emitting Lasers*, edited by R. Michalzik (Springer, Berlin, 2013).
- [4] H. Haken, *Light, Vol. 2 Laser Light Dynamics* (North-Holland, New York, 1985).
- [5] V. DeGiorgio and M. O. Scully, Analogy between the laser threshold region and a second-order phase transition, *Phys. Rev. A* **2**, 1170 (1970).
- [6] R. F. Oulton, V. J. Sorger, T. Zentgraf, R.-M. Ma, C. Gladden, L. Dai, G. Bartal, and X. Zhang, Plasmon lasers at deep subwavelength scale, *Nature* **461**, 629 (2009).
- [7] M. Khajavikha, A. Simic, M. Katz, J. H. Lee, B. Slutsky, A. Mizrahi, V. Lomakin, and Y. Fainman, Thresholdless nanoscale coaxial lasers, *Nature* **482**, 204 (2012).
- [8] D. Saxena, S. Mokkalapati, P. Parkinson, N. Jiang, Q. Gao, H. H. Tan and C. Jagadish, Optically pumped room-temperature GaAs nanowire lasers, *Nat. Photon.* **7**, 963 (2013).
- [9] S. T. Jagsch, et al., A quantum optical study of thresholdless lasing features in high- $\beta$  nitride nanobeam cavities, *Nat. Commun.* **9**, 564 (2018).
- [10] A. Bhattacharya, M. Zunaid Baten, I. Iorsh, T. Frost, A. Kavokin, and P. Bhattacharya, Room-temperature spin polariton diode laser, *Phys. Rev. Lett.* **119**, 067701 (2017).
- [11] R.-M. Ma and R. F. Oulton, Applications of nanolasers, *Nat. Nanotechnol.* **14**, 12 (2019).
- [12] I. Žutić, J. Fabian, and S. Das Sarma, Spintronics: Fundamentals and applications, *Rev. Mod. Phys.* **76**, 323 (2004).
- [13] N. Nishizawa, K. Nishibayashi, and H. Munekata, Pure circular polarization electroluminescence at room temperature with spin-polarized light-emitting diodes, *Proc. Nat. Acad. Sci.* **114**, 1783 (2017).
- [14] I. Žutić, G. Xu, M. Lindemann, P. E. Faria Junior, J. Lee, V. Labinac, K. Stojšić, G. M. Sipahi, M. R. Hofmann, and N. C. Gerhardt, Spin-lasers: spintronics beyond magnetoresistance, *Solid State Commun.* **316-317**, 113949 (2020).
- [15] I. V. Rozhansky, V. N. Mantsevich, N. S. Maslova, P. I. Arseyev, N. S. Averkiev, and E. Lähderanta, Ultrafast electrical control of optical polarization in hybrid semiconductor structure, *Physica E* **132**, 114755 (2021).
- [16] V. N. Mantsevich, I. V. Rozhansky, N. S. Maslova, P. I. Arseyev, N. S. Averkiev, and E. Lähderanta, Mechanism of ultrafast spin-polarization switching in nanostructures, *Phys. Rev. B* **99**, 115307 (2019).
- [17] N. Nishizawa and H. Munekata, Lateral-type spin-photonics devices: Development and applications, *Micromachines* **12**, 644 (2021).
- [18] E. Y. Tsymlal and I. Žutić (eds.), *Spintronics Handbook: Spin Transport and Magnetism*, 2nd ed. (CRC Press, Boca Raton, FL 2019).
- [19] H. Dery, Y. Song, P. Li, and I. Žutić, Silicon spin communication, *Appl. Phys. Lett.* **99**, 082502 (2011).
- [20] I. Žutić, A. Matos-Abiague, B. Scharf, H. Dery, and K. Belashchenko, Proximitized materials, *Mater. Today* **22**, 85 (2019).
- [21] A. Khaetskii, V. N. Golovach, X. Hu, and I. Žutić, Proposal for a phonon laser utilizing quantum-dot spin states, *Phys. Rev. Lett.* **111**, 186601 (2013).
- [22] S. Hallstein, J. D. Berger, M. Hilpert, H. C. Schneider, W. W. Rühle, F. Jahnke, S. W. Koch, H. M. Gibbs, G. Khitrova, M. Oestreich, Manifestation of coherent spin precession in stimulated semiconductor emission dynamics, *Phys. Rev. B* **56**, R7076 (1997).
- [23] H. Ando, T. Sogawa, and H. Gotoh, Photon-spin controlled lasing oscillations in surface-emitting lasers, *Appl. Phys. Lett.* **73**, 566 (1998).
- [24] J. Rudolph, D. Hägele, H. M. Gibbs, G. Khitrova, and M. Oestreich, Laser threshold reduction in a spintronic device, *Appl. Phys. Lett.* **82**, 4516 (2003).
- [25] J. Rudolph, S. Döhrmann, D. Hägele, M. Oestreich, and W. Stolz, Room-temperature threshold reduction in vertical-cavity surface-emitting lasers by injection of spin-polarized carriers, *Appl. Phys. Lett.* **87**, 241117 (2005).
- [26] M. Holub, J. Shin, and P. Bhattacharya, Electrical spin injection and threshold reduction in a semiconductor laser, *Phys. Rev. Lett.* **98**, 146603 (2007).
- [27] N. C. Gerhardt, S. Hövel, M. R. Hofmann, J. Yang, D. Reuter, A. Wieck, Enhancement of spin information with vertical cavity surface emitting lasers, *Electron. Lett.* **42**, 88 (2006).
- [28] S. Hövel, A. Bischoff, N. C. Gerhardt, M. R. Hofmann, T. Ackemann, A. Kroner, and R. Michalzik, Optical spin manipulation of electrically pumped vertical-cavity



- surface-emitting lasers, *Appl. Phys. Lett.* **92**, 041118 (2008).
- [29] D. Basu, D. Saha and P. Bhattacharya, Optical polarization modulation and gain anisotropy in an electrically injected spin laser, *Phys. Rev. Lett.* **102**, 093904 (2009).
- [30] D. Saha, D. Basu, and P. Bhattacharya, High-frequency dynamics of spin-polarized carriers and photons in a laser, *Phys. Rev. B* **82**, 205309 (2010).
- [31] M. Y. Li, H. Jähme, H. Soldat, N. C. Gerhardt, M. R. Hofmann, T. Ackemann, A. Kroner, and R. Michalzik, Birefringence controlled room-temperature picosecond spin dynamics close to the threshold of vertical-cavity surface-emitting laser devices, *Appl. Phys. Lett.* **97**, 191114 (2010).
- [32] N. C. Gerhardt, M. Y. Li, H. Jähme, H. Höpfner, T. Ackemann, and M. R. Hofmann, Ultrafast spin-induced polarization oscillations with tunable lifetime in vertical-cavity surface-emitting lasers, *Appl. Phys. Lett.* **99**, 151107 (2011).
- [33] S. Iba, S. Koh, K. Ikeda, and H. Kawaguchi, Room temperature circularly polarized lasing in an optically spin injected vertical-cavity surface-emitting laser with (110) GaAs quantum wells, *Appl. Phys. Lett.* **98**, 081113 (2011).
- [34] S. Iba, S. Koh, K. Ikeda, and H. Kawaguchi, Circularly polarized lasing over wide wavelength range in spin-controlled (110) vertical-cavity surface-emitting laser, *Solid State Commun.* **152**, 1518 (2012).
- [35] J. Frougier, G. Baili, M. Alouini, I. Sagnes, H. Y. Jaffrès, A. Garnache, C. Deranlot, D. Dolfi, and J.-M. George, Control of light polarization using optically spin-injected vertical external cavity surface emitting lasers, *Appl. Phys. Lett.* **103**, 252402 (2013).
- [36] J.-Y. Cheng, T.-M. Wond, C.-W. Chang, C.-Y. Dong, and Y.-F. Chen, Self-polarized spin-nanolasers, *Nat. Nanotechnol.* **9**, 845 (2014).
- [37] S. S. Alharthi, A. Hurtado, R. K. Al Seyab, V.-M. Korpjarvi, M. Guina, I. D. Henning, and M. J. Adams, Control of emitted light polarization in a 1310 nm dilute nitride spin-vertical cavity surface emitting laser subject to circularly polarized optical injection, *Appl. Phys. Lett.* **105**, 181106 (2014).
- [38] S. S. Alharthi, A. Hurtado, V.-M. Korpjarvi, M. Guina, I. D. Henning, and M. J. Adams, Circular polarization switching and bistability in an optically injected 1300 nm spin-vertical cavity surface emitting laser, *Appl. Phys. Lett.* **106**, 021117 (2015).
- [39] M. Lindemann, T. Pusch, R. Michalzik, N. C. Gerhardt, and M. R. Hofmann, Frequency tuning of polarization oscillations: Toward high-speed spin-lasers, *Appl. Phys. Lett.* **108**, 042404 (2016).
- [40] N. Yokota, R. Takeuchi, H. Yasaka, and K. Ikeda, Lasing polarization characteristics in 1.55- $\mu\text{m}$  spin-injected VCSELs, *IEEE Photon. Tech. Lett.* **29**, 711 (2017).
- [41] N. Yokota, and K. Nisaka, H. Yasaka, and K. Ikeda, Spin polarization modulation for high-speed vertical-cavity surface-emitting lasers, *Appl. Phys. Lett.* **113**, 171102 (2018).
- [42] M. Lindemann, G. Xu, T. Pusch, R. Michalzik, M. R. Hofmann, I. Žutić, and N. C. Gerhardt, Ultrafast spin-lasers, *Nature* **568**, 212 (2019).
- [43] C. Gøthgen, R. Oszwaldowski, A. Petrou, and I. Žutić, Analytical model of spin-polarized semiconductor lasers, *Appl. Phys. Lett.* **93**, 042513 (2008).
- [44] J. Lee, W. Falls, R. Oszwaldowski, and I. Žutić, Spin modulation in lasers, *Appl. Phys. Lett.* **97**, 041116 (2010).
- [45] J. Lee, R. Oszwaldowski, C. Gøthgen, and I. Žutić, Mapping between quantum dot and quantum well lasers: From conventional to spin lasers, *Phys. Rev. B* **85**, 045314 (2012).
- [46] J. Lee, S. Bearden, E. Wasner, and I. Žutić, Spin-lasers: From threshold reduction to large-signal analysis, *Appl. Phys. Lett.* **105**, 042411 (2014).
- [47] W. W. Chow and S. W. Koch, *Semiconductor-Laser Fundamentals: Physics of the Gain Materials*, (Springer, New York, 1999).
- [48] M. Holub and B. T. Jonker, Threshold current reduction in spin-polarized lasers: Role of strain and valence-band mixing, *Phys. Rev. B* **83**, 125309 (2011).
- [49] P. E. Faria Junior, G. Xu, J. Lee, N. C. Gerhardt, G. M. Sipahi, and I. Žutić, Towards high-frequency operation of spin-lasers, *Phys. Rev. B* **92**, 075311 (2015).
- [50] P. E. Faria Junior, G. Xu, Y.-F. Chen, G. M. Sipahi, and I. Žutić, Wurtzite spin lasers, *Phys. Rev. B* **95**, 115301 (2017).
- [51] G. Bourdon, I. Robert, I. Sagnes, and I. Abram, Spontaneous emission in highly excited semiconductors: Saturation of the radiative recombination rate, *J. Appl. Phys.* **92**, 6595 (2002). The linear form is obvious for  $T = 0$  K and  $n = p$ , where the density of electron-hole pairs that can recombine is  $n$ .
- [52] J. Hader, J. V. Moloney, and S. W. Koch, Beyond the ABC: carrier recombination in semiconductor lasers, *Proc. SPIE* **6115**, 61151T (2006). The precise functional form of the carrier recombination changes with density. At higher densities, commonly considered quadratic recombination,  $Bn^2$ , attains a linear form,  $Bn$ .
- [53] E. M. Purcell, Spontaneous emission probabilities at radio frequencies, *Phys. Rev.* **69**, 681 (1946).
- [54] P. A. Barnes and T. L. Paoli, Derivative measurements of the current-voltage characteristic of double-heterostructure injection lasers, *IEEE J. Quantum Electron.* **12**, 633 (1976).
- [55] T. L. Paoli, Determination of the lasing threshold in stripe-geometry double-heterostructure junction lasers, *Appl. Phys. Lett.* **29**, 673 (1976).
- [56] P. Westbergh, R. Safaisinia, E. Haglunda, J. S. Gustavson, A. Larsson, and A. Joel, High-speed 850 nm VCSELs with 28 GHz modulation bandwidth for short reach communication, *Proc. SPIE* **8639**, 8639X (2013).
- [57] S. F. Yu, *Analysis and Design of Vertical Cavity Surface Emitting Lasers*, (John Wiley & Sons, Inc., Hoboken, New Jersey, 2003).
- [58] N. C. Gerhardt, private communication.
- [59] S. Iba, Y. Ohno, and H. Saito, Recent progress on crystal growth of high-quality (110) GaAs-based quantum wells for spin laser, *Proc. SPIE* **11470**, 114702P (2020).
- [60] T. Pusch, E. La Tona, M. Lindemann, N. C. Gerhardt, M. R. Hofmann, and R. Michalzik, Monolithic vertical-cavity surface-emitting laser with thermally tunable birefringence, *Appl. Phys. Lett.* **110**, 151106 (2017).
- [61] T. Pusch, P. Debernardi, M. Lindemann, F. Erb, N. C. Gerhardt, M. R. Hofmann and R. Michalzik, Vertical-cavity surface-emitting laser with integrated surface grating for high birefringence splitting *Electron. Lett.* **55**, 1055 (2019).
- [62] T. Pusch, M. Lindemann, N. C. Gerhardt, M. R. Hofmann, and R. Michalzik, Vertical-cavity surface-emitting

- lasers with birefringence above 250 GHz, *Electron. Lett.* **51**, 1600 (2015).
- [63] M. Lindemann, N. Jung, P. Stadler, T. Pusch, R. Michalzik, M. R. Hofmann, and N. C. Gerhardt, Bias current and temperature dependence of polarization dynamics in spin-lasers with electrically tunable birefringence, *AIP Adv.* **10**, 035211 (2020).
- [64] T. Fördös, H. Y. Jaffrès, K. Postava, M. S. Seghilani, A. Garnache, J. Pistora, and H. J. Drouhin, Eigenmodes of spin vertical-cavity surface-emitting lasers with local linear birefringence and gain dichroism, *Phys. Rev. A* **96**, 043828 (2017).
- [65] N. Yokota and H. Yasaka, Spin laser local oscillators for homodyne detection in coherent optical communications, *Micromachines* **12**, 573 (2021).
- [66] M. Drong, T. Fördös, H. Y. Jaffrès, J. Peřina Jr., K. Postava, P. Ciompa, J. Piřtora, and H.-J. Drouhin, Spin-VCSELs with local optical anisotropies: Toward terahertz polarization modulation, *Phys. Rev. Applied* **15**, 014041 (2021).
- [67] M. San Miguel, Q. Feng, and J. V. Moloney, Light-polarization dynamics in surface-emitting semiconductor lasers, *Phys. Rev. A* **52**, 1728 (1995).
- [68] R. Al-Seyab, D. Alexandropoulos, I. D. Henning, and M. J. Adams, Instabilities in spin-polarized vertical-cavity surface-emitting lasers, *IEEE Photon. J.* **3**, 799 (2011).
- [69] M. Adams, N. Li, B. Cemlyn, H. Susanto, and I. Henning, Algebraic expressions for the polarisation response of spin-VCSELs, *Semicond. Sci. Technol.* **33**, 064002 (2018).
- [70] M. Drong, T. Fördös, H. Y. Jaffrès, J. Peřina Jr, K. Postava, J. Piřtora, and H.-J. Drouhin, Local and mean-field approaches for modeling semiconductor spin-lasers, *J. Opt.* **22**, 055001 (2020).
- [71] J. Frougier, G. Baili, I. Sagnes, D. Dolfi, J.-M. George, and M. Alouini, Accurate measurement of the residual birefringence in VECSEL: Towards understanding of the polarization behavior under spin-polarized pumping, *Opt. Expr.* **23**, 9573 (2015).
- [72] M. Alouini, J. Frougier, A. Joly, G. Baili, D. Dolfi, and J.-M. Georges, VSPIN: A new model relying on the vectorial description of the laser field for predicting the polarization dynamics of spin-injected V(e)CSELs, *Opt. Express* **26**, 6739 (2018).
- [73] Y. Ye, Z. J. Wong, X. Lu, X. Ni, H. Zhu, X. Chen, Y. Wang and X. Zhang, Monolayer excitonic laser, *Nat. Photon.* **9**, 733 (2015).
- [74] S. Wu, S. Buckley, J. R. Schaibley, L. Feng, J. Yan, D. G. Mandrus, F. Hatami, W. Yao, J. Vučković, A. Majumdar, and X. Xu, Monolayer semiconductor nanocavity lasers with ultralow thresholds, *Nature* **520**, 69 (2015).
- [75] C. Javerzac-Galy, A. Kumar, R. D. Schilling, N. Piro, S. Khorasani, M. Barbone, I. Goykhman, J. B. Khurgin, A. C. Ferrari, and T. J. Kippenberg, Excitonic emission of monolayer semiconductors near-field coupled to high-Q microresonators, *Nano Lett.* **18**, 3138 (2018).